

LOW TEMPERATURE, HIGH PERFORMANCE, PLANAR SOLID OXIDE FUEL CELLS AND STACKS

Anil V. Virkar (anil.virkar@m.cc.utah.edu Phone: (801) 581-5396),
Jai-Woh Kim (jkim@eng.utah.edu Phone: (801) 581-3148),
and
Karun Mehta (kmehta@eng.utah.edu Phone: (801) 581-3148)
Department of Materials Science & Engineering, 304 EMRO
University of Utah
Salt lake City, UT 84112

and

Kuan-Zong Fung (kfung@materialsys.com Phone: (801) 973-1199)
Materials and Systems Research, Inc.
1473 South Pioneer Road, Suite B
Salt lake city, UT 84104

ABSTRACT

Conversion of chemical energy of combustion of a fuel into electrical energy by fuel cells continues to be an important thrust area of energy conversion technology. Among these, fuel cells using either molten salt (MCFC) or solid oxide (SOFC) electrolytes are of particular interest because operation at higher temperatures allows for the use of natural gas as a fuel. High temperature fuel cells, however, are subject to materials-related problems such as corrosion which increase with temperature. In addition, the Nernst potential also decreases with increasing temperature. These two factors suggest that lowering of the operation temperature is preferred. However, higher operating temperatures are desirable for internal reforming as well as to minimize losses at electrolyte/electrode interfaces. Based on these considerations, a temperature range between ~600 and ~800°C is considered optimum. The focus of the present work has been on the development of solid oxide fuel cells made of thin electrolyte films supported on a relatively thick anode.

Anode-supported single cells of approximately 3 cm diameter with anode thickness of ~0.75 mm (750 μm), YSZ electrolyte thickness of ~10 μm , and LSM + YSZ cathode thickness of ~50 μm were fabricated. The cell fabrication procedure consists of depositing a thin film of YSZ by dip-coating on a powder compact of a mixture of nickel oxide and YSZ. Densification was achieved at a temperature below 1400°C. Single cells were tested between 650 and 800°C with humidified hydrogen as the fuel and air as the oxidant. Maximum power density at 800°C was 1.8 W/cm² (area specific resistance ~0.15 cm^2) and that at 650°C was 0.8 W/cm² (area specific resistance ~0.34 cm^2). The area specific resistance of the cells obeyed Arrhenius-type behavior with an activation energy of 50 kJ/mol. The observed behavior is in accord with the theoretical analysis of cell performance which takes into account transport of gaseous species through the porous electrodes.

For stack testing, square-shaped cells of dimensions 5 cm x 5 cm x ~2-3 mm were made. Four cell stacks with metallic interconnects were tested at 800°C. The interconnect was configured

from a commercial alloy foil of 5 mil thickness. The interconnect was subjected to surface treatments to improve its performance. No glass seal was used. The edges of the metallic interconnects serve as sealing gaskets. Manifolds were made of commercial alloys. The manifolds are spring-loaded against the stack with electrically insulating gaskets. The absence of a sealing glass allows one to disassemble the stack and reuse the same cells. Often, the same cells were used more than ten times. Also, the presence of a large amount of nickel in the anode renders the cells highly thermal shock-resistant. For example, a cell could be cooled from 800°C to room temperature within a few minutes. The typical repeat unit (anode-electrolyte-cathode-interconnect) area specific resistance was measured to be $\sim 0.5 \text{ cm}^2$. The cells used in this preliminary work were of a thickness much greater than the most optimum. Current efforts are directed towards lowering the thickness down to $\sim 1.5 \text{ mm}$.

Funded by Electric Power Research Institute (EPRI), Gas Research Institute (GRI), and the State of Utah.

I. INTRODUCTION

Fuel cells for direct conversion of chemical energy of a fuel into electrical energy is an important thrust area of energy conversion technology [1-7]. Among these, fuel cells using either molten salt or solid oxide electrolytes operate at high temperatures which allows for the use of natural gas as a fuel unlike low temperature PEM fuel cells which must use hydrogen. High temperature fuel cells, however, are not without drawbacks, the foremost being materials-related problems such as corrosion and/or oxidation. From the standpoint of direct utilization of natural gas as a fuel, there are two conflicting considerations. (1) Higher operating temperatures are preferred for internal reforming as well as for minimization of electrolyte/electrode interfacial losses, and (2) Lower operating temperatures are preferred for attaining a higher thermodynamic efficiency in addition to minimizing corrosion/degradation-related problems. Based on these factors, a temperature range between ~ 600 and $\sim 800^\circ\text{C}$ is considered to be optimum for high temperature fuel cells.

Much work has been reported on solid oxide fuel cells (SOFCs) over the past two decades. The commonly used solid electrolyte in SOFCs is yttria-stabilized zirconia (YSZ) which exhibits excellent stability and remains essentially a pure ionic conductor even in a reducing environment. At a given temperature, ionic conductivity of YSZ is lower than that of bismuth oxide or ceria which necessitates higher operating temperatures. Recently, however, there has been considerable effort devoted towards developing SOFCs for operation at temperatures lower than 800°C. If YSZ is used as the electrolyte, it is imperative that its thickness be made as small as possible. A thickness on the order of 10 μm is considered reasonable. Thin YSZ films, however, are not strong enough to be self-supporting and must be supported on either a porous anode or a cathode. In such cells, the ohmic contribution to the cell resistance can be made small. However, it is necessary that gas transport through the porous electrodes does not significantly add to the overall cell resistance. Thus, in electrode-supported cells, the electrode structure is an important design parameter.

The design of a high performance SOFC requires careful attention to the following parameters: (1) Ohmic contribution of the electrolyte and the electrodes, (2) Charge transfer or activation polarization, and (3) Mass transport through porous electrodes or concentration polarization. In SOFCs employing a thick electrolyte (typically $> 150 \mu\text{m}$) as the supporting member, the ohmic contribution is usually a significant part of the overall cell resistance. In addition, the activation overpotential may also be substantial. By contrast, in electrode-supported (either an anode or a cathode as the supporting structure) cells, a thin electrolyte (~ 10 to $30 \mu\text{m}$) is

deposited directly on a porous electrode. Thick porous electrodes additionally lower the activation overpotential or charge transfer resistance [9-11]. However, concentration polarization can be significant due to resistance to gas transport through porous electrodes. Thus, electrodes must be designed to minimize both activation as well as concentration polarizations through an analysis of charge transfer processes at electrode/electrolyte interfaces and transport of gases through porous electrodes. Such a design strategy was used in the present work for developing cells which are sufficiently thick to ensure excellent strength and durability, while still retaining high performance that can be achieved with thin, fragile cells. Excellent performance at the cell level is a necessary requirement for realizing high performance at the stack level, but by no means is sufficient. Issues regarding the type of interconnect used, interconnect properties concerning oxidation, and stacking strategy are equally important. In this work, efforts were also directed towards developing planar stacks using metallic interconnects.

II. EXPERIMENTAL PROCEDURE

Cell Fabrication: NiO and 8 mol.% yttria-stabilized zirconia (YSZ) powders obtained from commercial sources were mixed in desired proportions in ethanol for 24 hours. For single cell tests, discs of ~32 mm in diameter were die-pressed in a uniaxial press followed by isostatic pressing at pressures up to 200 MPa. For stack tests, square plates of dimensions 6 cm x 6 cm were pressed. Discs and plates were coated using a slurry of YSZ in ethanol, and later sintered in air at 1400°C for 1 hour. LSM powder of stoichiometry $\text{La}_{0.8}\text{Sr}_{0.2}\text{MnO}_{3-x}$ was prepared by calcining a mixture of La_2O_3 , SrCO_3 , and MnO_2 in air at 1000°C. The calcined LSM powder was subsequently ball-milled. A mixture containing LSM and YSZ powders in equal amounts (by weight) was made and mixed with an organic liquid to form a paste. The paste was applied over the sintered discs (on the dense YSZ layer). The discs were then heated to 400°C to burn out volatiles. This procedure was repeated until a layer of 50 to 70 μm thickness was formed. The discs were later heated to 1250°C for 1 hour. This thermal treatment was adequate to ensure the formation of a good bond between the porous LSM + YSZ cathode and the underlying dense YSZ layer, but not so severe as to form highly resistive pyrochlore phase, $\text{La}_2\text{Zr}_2\text{O}_7$. After electrochemical tests, the cells were fractured and examined under a scanning electron microscope. Selected samples of anodes were made with two types of YSZ powders; one containing 3 mol.% Y_2O_3 (tetragonal zirconia, TZP) and the other containing 8 mol.% Y_2O_3 (cubic zirconia). The objective was to determine flexural strength. Since the cells in the present work are anode-supported, it is important to ensure that the anode exhibits adequate strength. Samples containing varying amounts of NiO and zirconia were fabricated by conventional die-pressing, pressureless sintering in air followed by reduction in a hydrogen atmosphere at 800°C. Flexural strength was measured in four point bending.

Single Cell Testing: The single cell test stand consists of two alumina tubes in between which a cell can be secured. For single cell testing, disc-shaped cells were used. Silver meshes were used as current collectors which were pressed against the cathode and the anode with a thin layer of platinum resinates in between to ensure a good bond between the silver meshes and the electrodes. The cell was secured in two inconel bushings with an electrically insulating gasket. Silver current leads were affixed to the two silver meshes. The cell was placed inside a furnace. The test stand was designed in such a way that the seals (gaskets) were always under a spring loading with springs outside the furnace. Thus, no glass seal was necessary. This permitted repeated heating/cooling of the cells and retesting. Hydrogen as a fuel was bubbled through water maintained at a temperature ~33°C and air was circulated past the cathode. Temperature at the cell was varied between 650 and 800°C. Reduction of NiO into Ni was accomplished in-situ. Cell performance was measured using an electronic load.

Stack Testing: Several four cell stacks were assembled using metallic (superalloy) interconnect. Typical procedure for stack assembly and testing was as follows. End plates, which served as current collectors, were also made of a superalloy. The diameter of the current collector rods was 1.27 cm. Three voltage probes were introduced, one each attached to an interconnect. The stack was secured inside a metallic manifold with inert, insulating gaskets as edge seals. In order to improve the sealing, the stack was spring-loaded wherein the springs were outside the hot zone of the furnace. Stack was tested at 800°C with humidified hydrogen as the fuel and air as the oxidant. Reduction of NiO to Ni was achieved in-situ. The active area of the stack was estimated to be between 75 and 80 cm².

III. RESULTS AND DISCUSSION

Mechanical Properties of the Anode: In order that the cells can be handled without breakage, assembled in a stack, and survive during operation, it is imperative that at least one of the components comprising the cell, i.e., cathode, anode, or electrolyte must be of a sufficient thickness. The preferred choices include either the cathode as a support or the anode as a support, but not the electrolyte since the ohmic contribution is substantial, especially with YSZ as the electrolyte and at temperatures below about 950°C. Figure #1 shows the results of strength vs. nickel content of zirconia + nickel bar-shaped samples made with 3 mol.% Y₂O₃-doped ZrO₂ (TZP) and 8 mol.% Y₂O₃-doped ZrO₂ powder. The numbers in parentheses indicate the porosity. Note that the strength of Ni + TZP is considerably higher than that of Ni + YSZ. Also, it is observed that the strength of Ni + TZP decreases with increasing Ni content while that of Ni + YSZ increases over the range studied. The possible reason is that the intrinsic strength of Ni may be greater than that of YSZ but less than that of TZP. A few samples of LSM with 25% porosity were also tested for strength. Strength of LSM was measured to be about ~50 MPa. Note that the strength of Ni + zirconia is considerably greater than that of LSM. Since the ionic conductivity of YSZ is greater than that of TZP, and that YSZ is not sensitive to low temperature strength degradation, unlike TZP, in the present work anodes were made of Ni + YSZ.

Issues Concerning Delamination: From the standpoint of mismatch of thermal expansion stresses, it would appear the choice should be LSM as the support structure. This is because the coefficient of thermal expansion of YSZ is better matched with LSM instead of Ni + zirconia. Fortunately, YSZ has a lower coefficient of thermal expansion compared to Ni + zirconia. Thus, the YSZ film at room temperature is under compression and thus should not crack. It can, however, delaminate. The tendency for delamination is a function of $\frac{\alpha_2 - \alpha_1}{t} (T_i - T_o)$, where α_2 is the difference in coefficients of thermal expansion and T is the temperature differential from the temperature at which stresses are zero (stress relief temperature) and the test temperature, and the thickness of the film. It can be shown that the thinner the film, the less likely it is to delaminate [8,9]. In addition, at the operating temperature T is rather small. Propensity for delamination can be assessed via a schematic shown in Figure #2. Since the cathode is highly porous, its effect on the delamination calculations can be ignored in a first order calculation. It can be shown that delamination due to thermal stresses can occur provided [8,9],

$$(\alpha_2 - \alpha_1)(T_i - T_o) = \frac{1}{t} \sqrt{\frac{2 \gamma_{fm} (1 - \nu_1^2)}{E_1}} \quad (1)$$

where α_2 and α_1 are thermal expansion coefficients of the Ni + YSZ anode and YSZ film, respectively, T_i is the temperature above which stress relief by creep can readily occur, T_o is room temperature (for delamination at room temperature) or service temperature (for delamination at service temperature), γ_{fm} is the interfacial fracture energy, ν_1 is the Poisson's

ratio of YSZ (film), E_1 is the Young's modulus of YSZ, and t is the YSZ film thickness. Alternatively, YSZ films of a thickness smaller than a critical thickness, t_{cr} , given by

$$t_{cr} = \frac{2 \gamma_{fm} (1 - \nu^2)}{E_1 (\alpha)^2 (T)^2} \quad (2)$$

will not delaminate. The preceding assumes that the thickness of the Ni + YSZ anode is much greater than that of the YSZ film, i.e. $d \gg t$. Based on the known values of thermal expansion coefficients, elastic properties of nickel and zirconia, and an assumed interfacial energy of 20 J/m², it is estimated that t_{cr} is at least on the order of 30 to 40 μm for volume fractions of nickel and YSZ in the anodes of the present work. Thus, as long as the YSZ film thickness is smaller than 30 to 40 μm , delamination is not expected at room temperature. In the present work, typical thickness of the YSZ film was 10 to 15 μm . No delamination has been observed, in accord with calculations.

Issues Concerning Electrode Thickness: Effective Charge Transfer Resistance: Both electrodes in the present work consisted of a mixture of an electrocatalyst (Ni for the anode, LSM for the cathode) and YSZ. It is known that composite electrodes exhibit lower overpotentials [10-12]. The presence of YSZ in addition to the electrocatalyst increases the three phase boundary (TPB) length, provides parallel path for oxygen ions and thereby spreads the reaction zone into the electrodes. Recent work has shown that the effective charge transfer resistance can be given in terms of the various parameters of the electrodes [12]. Figure #3 shows a schematic of a cell in which porous composite electrodes are shown separated by a dense YSZ electrolyte membrane. The effective charge transfer resistance, R_{ct}^{eff} , is given as a function of electrode thickness, h , by [12]

$$R_{ct}^{eff} = \frac{BR_{ct}}{\frac{1 + e^{-\frac{h}{2\lambda}}}{1 + e^{-\frac{h}{\lambda}}} (1 - \beta) B e^{-\frac{h}{\lambda}} + \frac{1 + e^{-\frac{h}{2\lambda}}}{1 + e^{-\frac{h}{\lambda}}} (1 - e^{-\frac{h}{\lambda}}) + B} \quad (3)$$

where

$$\lambda = \sqrt{\frac{R_{ct}}{\sigma_i (1 - \beta)}} \quad \text{and} \quad \beta = \frac{R_{ct}}{R_{ct} + B} \quad (4)$$

It can be shown that as $h \rightarrow \infty$, the R_{ct}^{eff} is given by [12]

$$R_{ct}^{eff} = \sqrt{\frac{BR_{ct}}{\sigma_i (1 - \beta)}} \quad (5)$$

Equation (3) shows that the R_{ct}^{eff} depends upon a number of parameters including the electrode thickness, h , in a complicated manner. However, the asymptotic limit given by equation (5) as $h \rightarrow \infty$ has a simple appearance. It is seen that R_{ct}^{eff} exhibits an inverse square root dependence on the ionic conductivity, σ_i , of the electrolyte (YSZ) part of the electrolyte, square root dependence on the intrinsic charge transfer resistance, R_{ct} , and square root dependence on the microstructural parameter, B , of the electrode. Calculations show that typically the asymptotic limit is reached in about 30 to 100 μm of thickness, h . Calculations further show that for an electrode of $h = 50 \mu\text{m}$, with an $R_{ct} = 2.4 \text{ cm}^2$, it is possible to achieve R_{ct}^{eff} values on the order of 0.1 cm^2 , i.e., over twenty times reduction in charge transfer resistance. These considerations were used in the design of electrodes.

Issues Concerning Electrode Thickness: Concentration Polarization: Mass transport of gaseous species through the electrodes was carefully analyzed in order to achieve the desired porosity and electrode morphology. These considerations were important in designing electrodes to minimize concentration polarization.

Single Cell Testing: Typical thicknesses of cathode, electrolyte, and anode were respectively $\sim 50 \mu\text{m}$, $\sim 10 \mu\text{m}$, and $\sim 750 \mu\text{m}$. The anode porosity was measured to be 38 vol.%. Cathode porosity was not measured on this cell but was estimated to be about 30 vol.% based on measurements made on thicker LSM + YSZ cathodes made separately. Figure #4(a) shows the results on one of the cells in which the voltage is plotted vs. current density at four temperatures; 650, 700, 750, and 800°C. The short circuit current density at 800°C was in excess of 5.5 A/cm² and that at 650°C was in excess of 3 A/cm². The voltage vs. current density trace exhibits an initial concave-up curvature followed by an approximately linear behavior, followed by a convex-up curvature at higher current densities. This trend was particularly more pronounced at higher temperatures. Slopes of linear regions of the voltage vs. current density plots were estimated at the four temperatures. This slope yields effectively the area specific cell resistance, R_{cell} , predominantly the ohmic contribution. The R_{cell} should contain at a minimum the area specific resistance of the electrolyte, $i t$, where i which is

$= \frac{1}{i}$, is the electrolyte resistivity and t is the electrolyte thickness. Table 1 gives the

experimentally measured conductivity of a YSZ disc of 2 mm thickness at the four temperatures at which the cell performance was measured. Also given in the table is the estimated electrolyte contribution to the R_{cell} as well as the measured (minimum) R_{cell} from linear parts of the voltage vs. current density plots. R_{cell} would also be expected to contain the ohmic part of the activation overpotential or the charge transfer resistance in addition to the ohmic part of the concentration polarization. The inset shows a plot of $\ln(R_{cell} / T)$ vs. $1/T$, where T is the temperature in K, from the slope of which, an activation energy, Q_{cell} of ~ 50 kJ/mol. is measured. The difference between R_{cell} and $i t$ is approximately the contribution of charge transfer and concentration polarization. This is also listed in Table 1. It is seen that $(R_{cell} - R_{electrolyte})$ over a range of temperatures from 700 to 800°C is between ~ 0.04 and 0.07

cm², showing that the combined contribution of activation and concentration polarizations is typically less than the ohmic contribution. At 650°C, the estimated $(R_{cell} - R_{electrolyte})$ is only about 0.007 cm². We believe such a low value simply reflects an error due to possible differences between the actual ohmic contribution in the cell and that estimated based on measurements of conductivity made on a thick pellet. The ionic conductivity of the thin film YSZ in the actual cell may have been higher than the thick disc due to some differences in the microstructure, e.g. the grain size or differences in the grain boundary structure/chemistry. Nevertheless, the results show that in the anode-supported cells made in the present work, the combined contribution of activation and concentration polarizations has been substantially lowered compared to some of the work reported on electrolyte-supported cells.

Figure #4(b) shows the corresponding plots of power density vs. current density at various temperatures. The maximum power density measured at 800°C was ~ 1.8 W/cm² and that measured at 650°C was ~ 0.82 W/cm². It is seen that power density vs. current density plot becomes increasingly nonsymmetric with increasing temperature. This behavior is consistent with calculations based on transport of gaseous species through porous electrodes.

In order to assess the thermal shock behavior of anode-supported cells, the following experiments were performed. Some of the cells of dimensions ~ 5 cm x ~ 5 cm and ~ 2 - 3 mm in thickness, that had been heat treated in hydrogen to convert NiO into Ni, were heated in an inert atmosphere to 800°C (to prevent the oxidation of Ni). Then, while still hot, the cells were removed from the furnace and placed on a ceramic plate at room temperature. The cells did not crack and the YSZ electrolyte did not debond indicating that the thermal shock resistance of these anode-supported cells is excellent.

Stack results: Stack testing was conducted at 800°C using cells of typical dimensions ~ 5 cm x ~ 5 cm x ~ 2 - 3 mm. Each stack tested had four cells separated by metallic interconnects. The interconnect was subjected to surface treatments to minimize the effects of oxidation. The best interconnect material explored to date exhibits an area specific resistance of ~ 0.08 cm^2 after 5,000 hours at 800°C . Performance is expected to be better at a lower temperature such as 650°C . Voltage probes were introduced between each repeat unit. No glass was used; the edges of the interconnects themselves served as seals. Manifolds were made of a metallic alloy which were attached using electrically insulating inorganic gaskets.

Figure #5 shows voltage vs. current for the four repeat units of the stack. Note that the repeat unit area specific resistance, including the interconnect, is as low as ~ 0.49 cm^2 . Figure #6 shows a plot of the total power vs. current. The maximum power measured was ~ 33 watts. The thickness of the repeat unit was about 3 mm. This translates into a volumetric power density of 1.1 kW/liter (excluding manifolding) at 800°C . The cells used were not the most advanced ones incorporating recent improvements in electrode design. It is anticipated that with further improvements in cell fabrication procedures and interconnect, significantly higher stack performance should be possible. Figure #7 shows stack performance history of our work.

SUMMARY

Anode-supported single cells with YSZ as the electrolyte and LSM + YSZ as the cathode were fabricated and tested. Maximum power densities as high 1.8 W/cm^2 at 800°C and 0.82 W/cm^2 at 650°C were measured with humidified hydrogen as the fuel and air as the oxidant. At 800°C , the lowest area specific resistance measured was ~ 0.13 cm^2 in the ohmic regime. The design of the electrode involved attention to both charge transfer processes at electrolyte/electrode interfaces as well as gas transport through porous electrodes. Four cell stacks using square cells of dimensions 5 cm x 5 cm were assembled and tested using metallic interconnects. Critical issues concerning the metallic interconnect involved oxidation resistance of the alloys and the electronic conductivity of the oxide scale. Four cell stacks tested exhibited area specific repeat unit as low as 0.5 cm^2 at 800°C . The cells tested were not the highest performing cells. Even with these cells of intermediate level performance, stack power of 33 watts was measured which translates into ~ 1.1 kW/liter at 800°C .

References:

- 1) Proceedings of the Third International Symposium on 'Solid Oxide Fuel Cells', The Electrochemical Society, Inc., Pennington, NJ, (1993).
- 2) Proceedings of the Fourth International Symposium on 'Solid Oxide Fuel Cells', The Electrochemical Society, Inc., Pennington, NJ, (1995).
- 3) '1992 Fuel Cell Seminar'. November 29 - December 2, 1992, Tucson, AZ. Sponsored by the Fuel Cell Seminar Organizing Committee.
- 4) '1994 Fuel Cell Seminar'. November 28 - December 1, 1994, San Diego, CA. Sponsored by the Fuel Cell Seminar Organizing Committee.
- 5) '1996 Fuel Cell Seminar', November 1996, Orlando, FL. Sponsored by the Fuel Cell Organizing Committee.
- 6) N. Q. Minh, *J. Am. Ceram. Soc.*, **76** 563 (1993).
- 7) 'Fuel Cells: A Handbook' (Revision 3), U. S. Department of Energy, METC, J. H. Hirschenhofer, D. B. Stauffer, and R. R. Engleman, January 1994.
- 8) G. P. Cherepanov, 'Mechanics of Brittle Fracture', McGraw-Hill, New York, (1973).
- 9) A. V. Virkar, unpublished work, (1992).
- 10) T. Kenjo, S. Osawa, and K. Fujikawa, *J. Electrochem. Soc.*, **138** 349 (1991).
- 11) T. Kenjo and M. Nishiya, *Solid State Ionics*, **57** 295 (1992).
- 12) C. W. tanner, K-Z Fung, and A. V. Virkar, *J. Electrochem. Soc.*, **144** [1] 21-30 (1997).

Table 1

Temperature (°C)	Electrolyte Resistivity, i (cm)	Calculated $R_{electrolyte} = \frac{t}{i}$ (cm ²)	Measured R_{cell} (cm ²)	$R_{cell} - R_{electrolyte}$ (Contributions from activation and concentration polarizations)
650	248	0.248	0.255	0.007
700	147	0.147	0.189	0.042
750	91	0.091	0.151	0.06
800	61	0.061	0.130	0.069

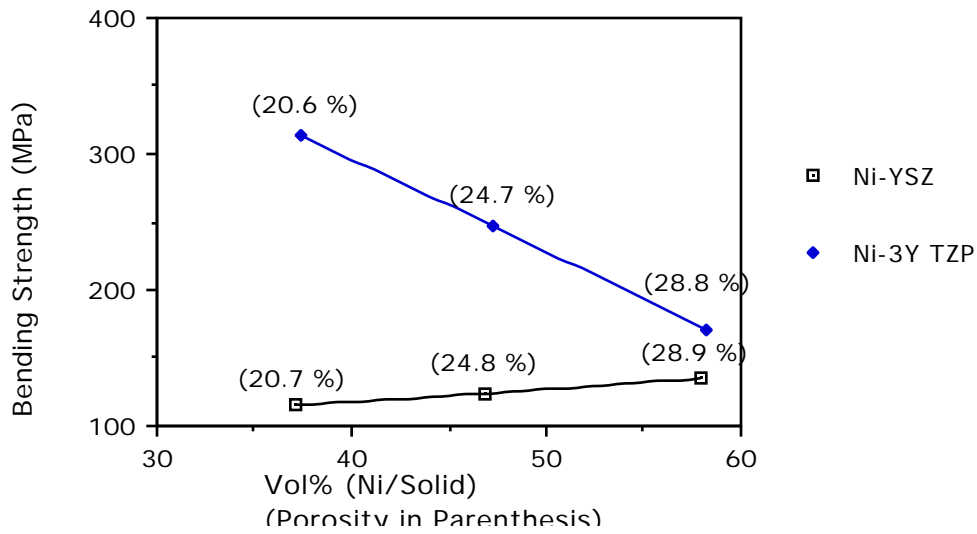


Figure #1: Flexural strength measured on Ni + 8 mol.% Y_2O_3 -doped ZrO_2 (YSZ) and Ni + 3 mol. % Y_2O_3 -doped ZrO_2 (TZP) as a function of vol.% Ni. The porosity is given in parentheses.

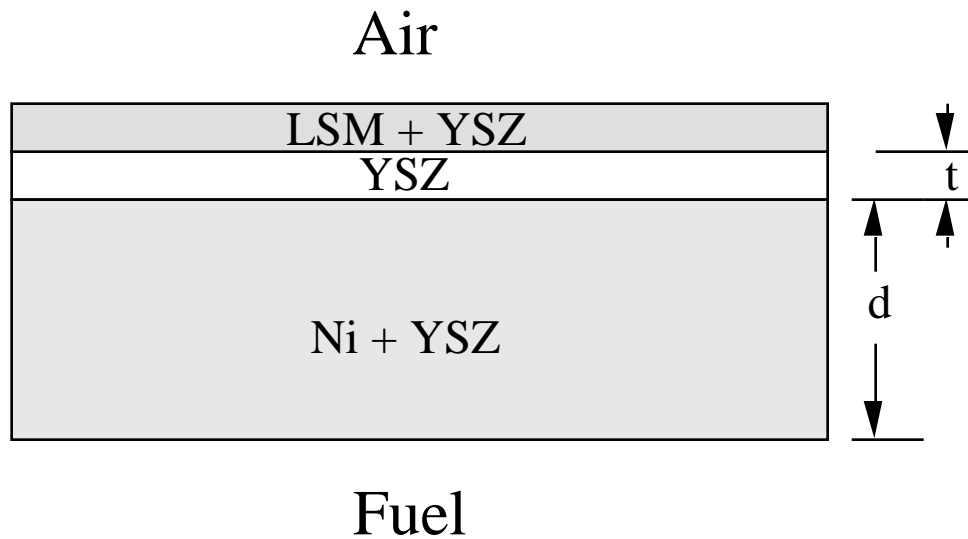


Figure #2: A schematic showing an anode-supported cell. Since the LSM + YSZ cathode is porous, its Young's modulus is rather small. Thus, calculations of stresses to assess potential for delamination was based on YSZ film thickness alone.

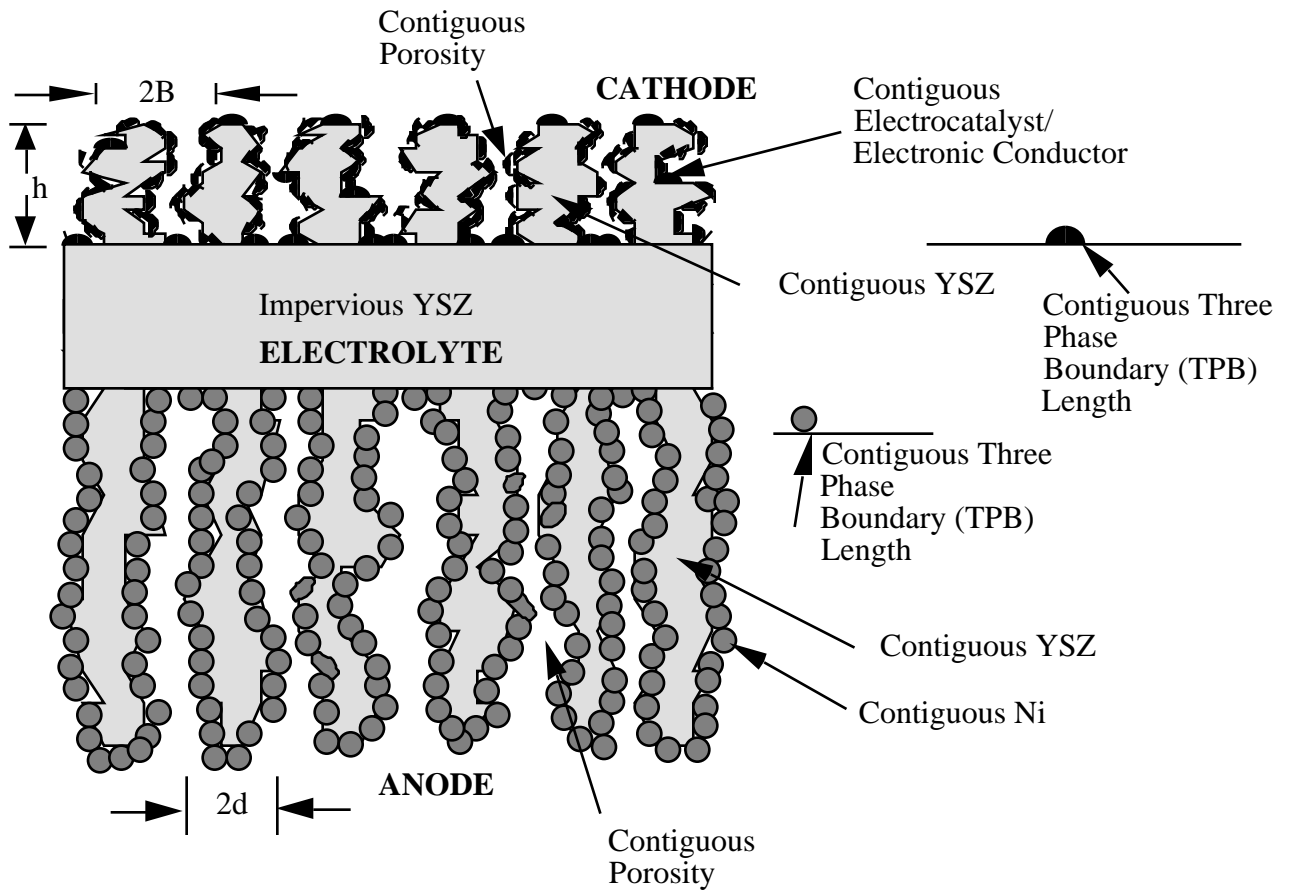


Figure #3: A schematic of an anode-supported cell showing contiguous YSZ in both electrodes, contiguous electrocatalyst in both electrodes, contiguous porosity in both electrodes, and a large TPB length in both electrodes.

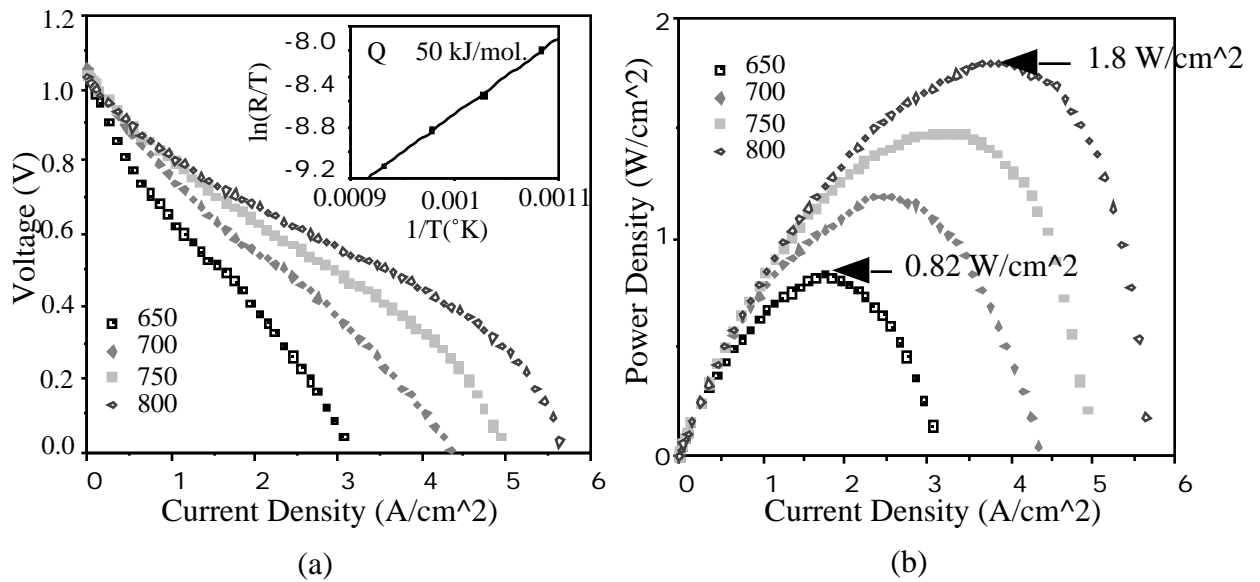


Figure #4 Voltage and power density vs. current density plots on a single cell at various temperatures. The maximum power densities at 650 and 800 °C measured were ~ 0.82 and ~ 1.8 W/cm² with humidified hydrogen as the fuel and air as the oxidant. Cell dimensions: Cathode thickness 50 μ m, electrolyte thickness 10 μ m, and the anode thickness 750 μ m (0.75 mm). Inset in (a) shows an Arrhenius plot of the cell resistance (determined from the linear part of the voltage vs. current density traces) as a function of temperature. The overall cell resistance obeys an Arrhenius behavior with an activation energy, $Q = 50$ kJ/mol.

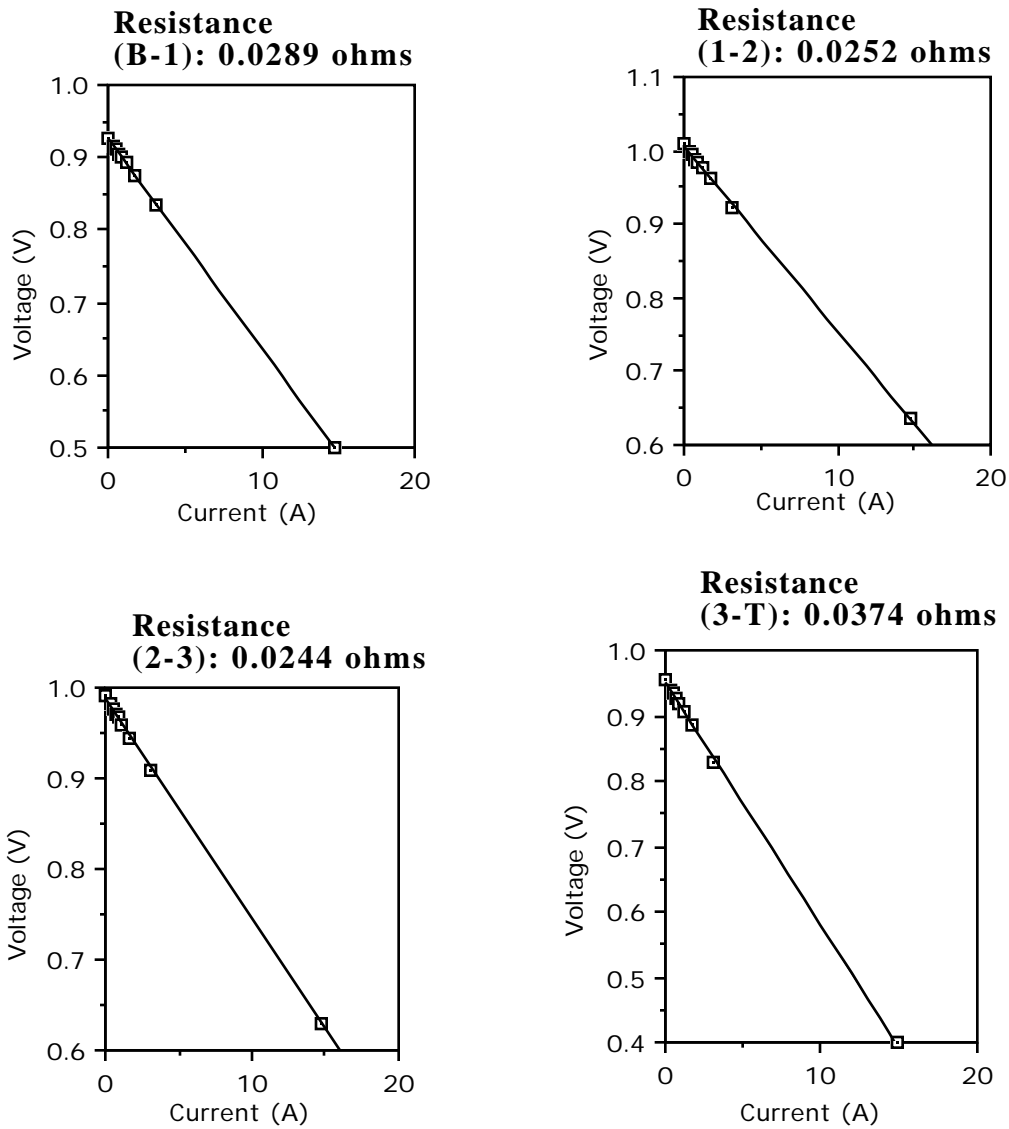


Figure #5: Voltage vs. current traces for the repeat units of a four cell stack tested at 800°C with humidified hydrogen as the fuel and air as the oxidant. Area per cell was $\sim 20 \text{ cm}^2$. The area specific resistance for (1-2) and (2-3) repeat units were 0.5 cm^2 . Slightly higher values for the bottom current collector and cell #1 (B-1) and top current collector and cell #3 (T-3) are due to somewhat poorer contact between the cell and the current collectors. The above shows that the cell to cell contact (through the metallic interconnect) is quite good.

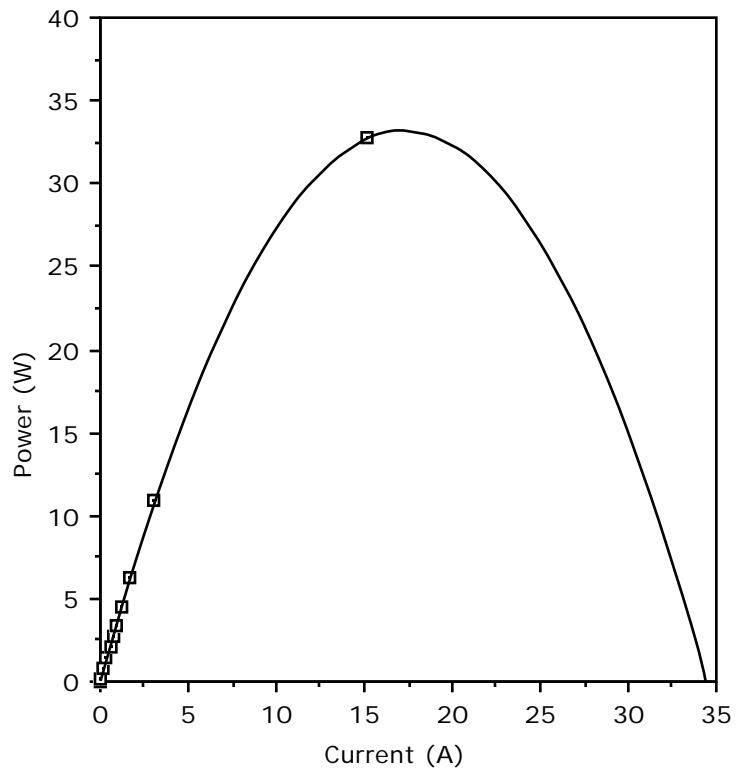


Figure #6: Power vs. current for a four cell stack tested at 800°C with a metallic interconnect.

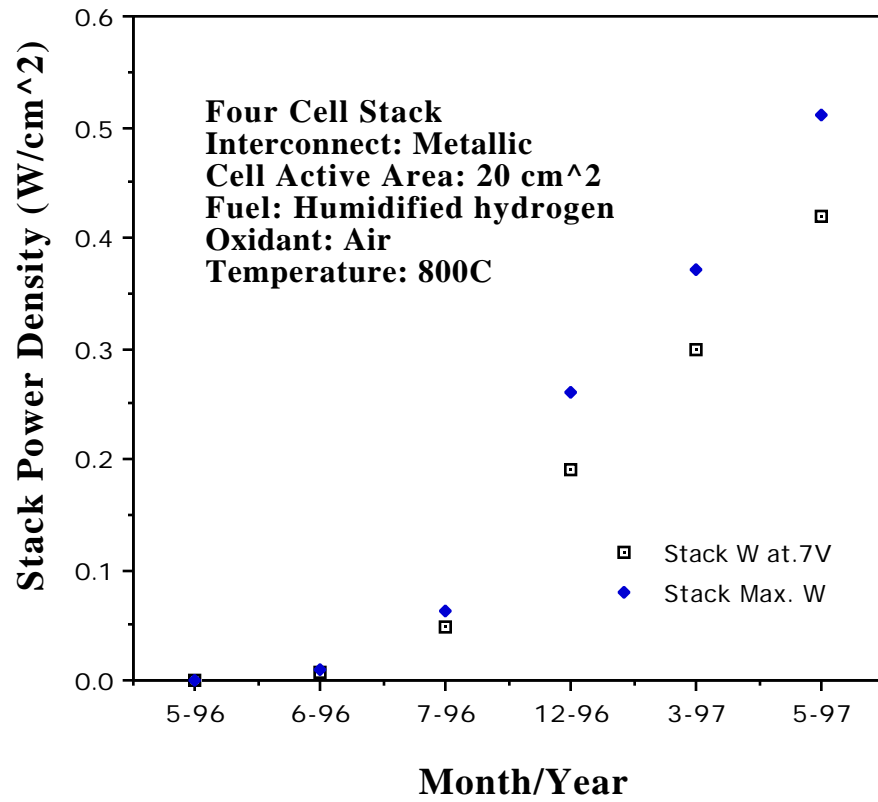


Figure #7: Stack performance history.